

## Structural and Molecular Insight into Resistance Mechanisms of First Generation cMET Inhibitors

Gavin W. Collie,<sup>\*,†</sup> Cheryl M. Koh,<sup>‡,⊥</sup> Daniel J. O'Neill,<sup>†</sup> Christopher J. Stubbs,<sup>†</sup> Puneet Khurana,<sup>†</sup> Alice Eddershaw,<sup>†</sup> Arjan Snijder,<sup>§</sup> Fredrik Mauritzson,<sup>§</sup> Louise Barlind,<sup>§</sup> Ian L. Dale,<sup>†</sup> Joseph Shaw,<sup>†</sup> Christopher Phillips,<sup>†</sup> Edward J. Hennessy,<sup>||,#</sup> Tony Cheung,<sup>||</sup> and Ana J. Narvaez<sup>\*,†</sup>

<sup>†</sup>Discovery Sciences, R&D, AstraZeneca, Cambridge, U.K.

<sup>‡</sup>Discovery Sciences, R&D, AstraZeneca, Waltham, Massachusetts 02451, United States

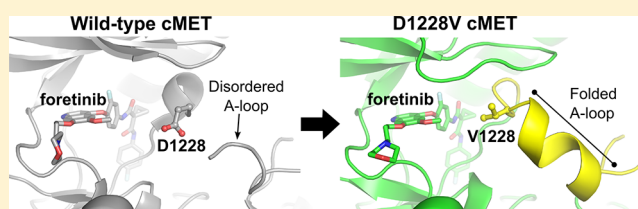
<sup>§</sup>Discovery Sciences, R&D, AstraZeneca, Gothenburg, Sweden

<sup>||</sup>Oncology, R&D, AstraZeneca, Waltham, Massachusetts 02451, United States

### Supporting Information

**ABSTRACT:** Many small molecule inhibitors of the cMET receptor tyrosine kinase have been evaluated in clinical trials for the treatment of cancer and resistance-conferring mutations of cMET are beginning to be reported for a number of such compounds. There is now a need to understand specific cMET mutations at the molecular level, particularly concerning small molecule recognition. Toward this end, we report here the first crystal structures of the recent clinically observed resistance-conferring D1228V cMET mutant in complex with small molecule inhibitors, along with a crystal structure of wild-type cMET bound by the clinical compound savolitinib and supporting cellular, biochemical, and biophysical data. Our findings indicate that the D1228V alteration induces conformational changes in the kinase, which could have implications for small molecule inhibitor design. The data we report here increases our molecular understanding of the D1228V cMET mutation and provides insight for future inhibitor design.

**KEYWORDS:** cMET, kinase, drug resistance, small molecule inhibitor, X-ray crystallography



The cMET receptor tyrosine kinase plays a key role in cell proliferation, survival, motility, and angiogenesis, and as such, has been found to be dysregulated in a large number of cancers, including those with poor outcomes such as papillary renal cell carcinoma and non-small cell lung carcinoma (NSCLC).<sup>1</sup> While cMET is well-known to be a major driver of many tumors, it also plays a key role in the emergence of resistance to targeted NSCLC therapies. Currently, there is no cure available for advanced NSCLC, and the majority of patients develop resistance to their treatment.<sup>2,3</sup> In advanced epidermal growth factor (EGFR)-mutated NSCLC, the most common acquired resistance mechanism to first-line treatment with early generation tyrosine kinase inhibitors (TKIs) is the T790M EGFR mutation.<sup>4,5</sup> Osimertinib, a third-generation EGFR-TKI, potently and selectively inhibits both EGFR-TKI sensitizing and T790M resistance mutations, and is more efficacious than the earlier generation EGFR-TKIs.<sup>6,7</sup> Recent preliminary data show that acquired cMET amplifications are the main resistance mechanism to first- and second-line treatment with osimertinib in patients with advanced NSCLC.<sup>8,9</sup> To overcome this cMET-driven resistance, the combination of osimertinib and savolitinib, a cMET inhibitor, is being explored in clinical trials.<sup>10,11</sup>

cMET therefore plays a key role as both a tumor driver and as a mechanism of TKI resistance, and a significant number of

cMET-targeted small molecule inhibitors have been assessed in the clinic.<sup>12</sup> Many of these small molecules, and in particular those belonging to the “type-I” inhibitor class such as savolitinib, are highly selective for cMET over other kinases<sup>13,14</sup> (Figure 1). The selectivity of these compounds is driven by a key  $\pi$ -stacking interaction between inhibitor aromatic groups and a tyrosine residue (Y1230) located within the activation loop (A-loop) of the kinase. However, resistance-conferring point mutations of cMET—presumed to act by directly or indirectly disrupting this key  $\pi$ -stacking interaction—have recently been reported in the clinic in patients treated with such cMET-selective type-I compounds, including crizotinib and savolitinib. The type II compound class tend to have a broader activity spectrum with the potential to overcome the acquired resistance to type I inhibitors,<sup>15</sup> but with an expected increased tolerability burden.<sup>16</sup>

Savolitinib is an exquisitely selective cMET inhibitor,<sup>14</sup> which has recently shown promising safety and antitumor activity in the clinic.<sup>10,11,17</sup> However, as found with all therapies in the advanced NSCLC setting, patients ultimately

Received: June 21, 2019

Accepted: August 2, 2019

Published: August 2, 2019

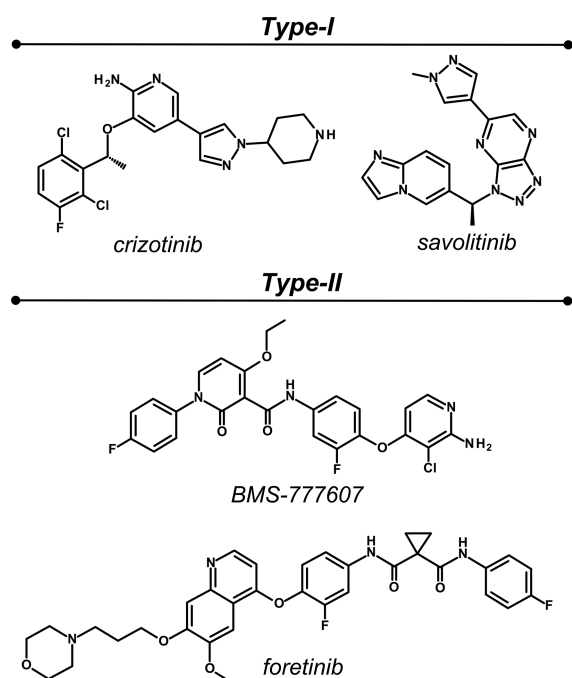


**Figure 1.** Type-I (crizotinib<sup>13</sup> and savolitinib<sup>14</sup>) and type-II (foretinib<sup>30</sup> and BMS-777607<sup>31</sup>) small molecule cMET inhibitors studied in this work.

develop therapeutic resistance. Resistance mechanisms can be described as on-target, preventing drug binding, or bypass, where the tumor cell has established an alternative proliferative drive that overcomes target inhibition. On-target cMET mutations have been reported in case studies for crizotinib, including Y1230H/C, D1228N/H, and D1231Y single-point alterations in NSCLC,<sup>18–23</sup> and a D1228V mutation for a NSCLC patient treated with savolitinib and osimertinib, following progression on initial treatment with erlotinib.<sup>16</sup>

While much is known concerning a number of these (and other) cMET mutations,<sup>24–28</sup> structural data is almost non-existent,<sup>29</sup> and to our knowledge, the D1228V cMET mutant has received little attention. Here, we report structural, cellular, biochemical, and biophysical studies of the D1228V cMET mutant with a view to understanding this mutation with respect to small molecule inhibition and molecular resistance.

We first sought to characterize the cellular effects of the D1228V cMET mutant within the context of small molecule inhibition. A previous study of the D1228V cMET mutant using HEK 293T and PC9 cells showed this mutation to abolish the activity of savolitinib, yet the activity of the type-II cMET inhibitor cabozantinib was retained.<sup>16</sup> Type-II kinase inhibitors typically do not rely on interactions with A-loop residues (such as D1228 or Y1230 of cMET) for binding; thus, a number of such compounds are active against cMET harboring A-loop mutations.<sup>16,24</sup> To investigate the cellular effects of the D1228V cMET mutant further, we used CRISPR/Cas9 methods to generate an isogenic model of acquired savolitinib resistance by knocking the D1228V cMET mutation into cMET-amplified H1993 cells, a NSCLC cell line (see [Supporting Information](#) for further details). Growth inhibition studies using the parental (i.e., wild-type) H1993 cells treated with either savolitinib or the type-II compound foretinib<sup>30</sup> (Figure 1) showed this wild-type cell line to be sensitive to both compounds, with pGI<sub>50</sub> (pGI<sub>50</sub> = -log<sub>10</sub>(GI<sub>50</sub>), M) values of 8.03 and 7.21 for savolitinib and foretinib, respectively (Figure 2a–b and Table S1). In contrast, the H1993 D1228V cMET cells were sensitive to foretinib (pGI<sub>50</sub> = 7.28) but not to savolitinib (pGI<sub>50</sub> = 5.08), with a greater than 800-fold loss in sensitivity to savolitinib compared to the parental cell line. Analysis of cMET activation and downstream signaling components indicated that in the parental H1993 cells, phospho-cMET (pMET) was abolished by both savolitinib and foretinib treatment, followed by a reduction of phospho-AKT (pAKT) levels (Figure 2c). In

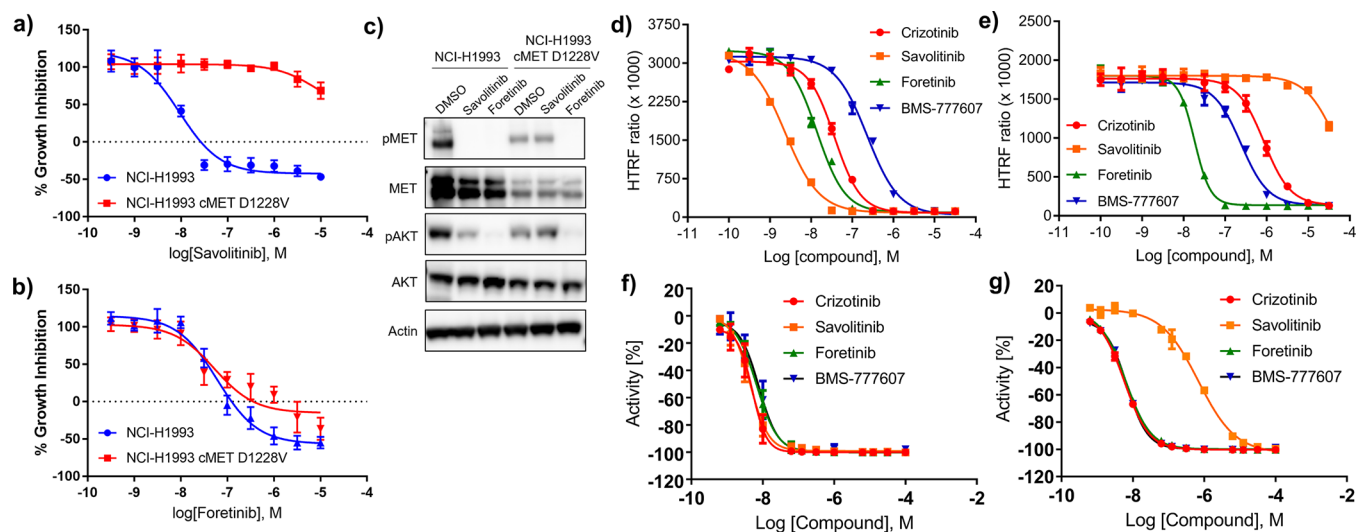


**Figure 2.** Cellular and *in vitro* small molecule inhibition studies of wild-type and D1228V cMET. (a–b) Growth inhibition studies (three-day proliferation assay) of savolitinib (a) and foretinib (b) using parental NCI-H1993 cells (blue trace) and CRISPR/Cas9 modified NCI-H1993 cells expressing D1228V cMET (red trace). Values shown are average of three separate experiments. (c) Western blot analysis of NCI-H1993 and NCI-H1993 D1228V cMET cells treated with 1 μM savolitinib or foretinib for 4 h. (d–e) HTRF-based assessment of four small molecules in NCI-H1993 cells (d) and NCI-H1993 D1228V cMET cells (e). (f–g) Enzyme inhibition studies of four small molecules using wild-type (f) or D1228V (g) cMET. All potencies determined from these experiments except that determined for savolitinib in panel (g) are beyond the theoretical tight binding limit of the assay. Further experimental details can be found in Table S1 and in the [Supporting Information](#).

contrast, the H1993 D1228V cMET cells treated with savolitinib showed no reduction in pMET or pAKT levels, while these markers remained sensitive to foretinib (Figure 2c).

We next used a cellular homogeneous time-resolved FRET (HTRF) system to investigate the D1228V cMET mutant further and to allow us to expand the range of compounds studied. Parental H1993 and H1993 D1228V cMET cells were incubated with savolitinib for 4 h followed by fluorescence detection of pMET (residues Y1234/Y1235), revealing the single-digit nanomolar activity of savolitinib in wild-type H1993 cells ( $pIC_{50} = 8.70$  [ $pIC_{50} = -\log_{10}(IC_{50}, M)pIC_{50} < 4.5$ ) (Figure 2d–e and Table S1). Interestingly, analysis of a second type-I compound, crizotinib,<sup>13</sup> showed that, although over 10-fold less active than savolitinib in the parental H1993 cells, the drop-off from parental to D1228V cMET was considerably less pronounced for this compound than observed for savolitinib (Figure 2d–e and Table S1). Two type-II compounds—foretinib<sup>30</sup> and BMS-777607<sup>31</sup>—were also analyzed using this HTRF system, with both compounds seen to be equally active against both parental H1993 and H1993 D1228V cMET cells, with  $pIC_{50}$  values in the range of 6.67–7.91 (Figure 2d–e and Table S1). Collectively, these findings indicate that the D1228V cMET mutation leads to resistance to type-I inhibitors (particularly savolitinib) but not to type-II inhibitors, in line with data reported previously concerning this mutant.<sup>16</sup>

We next tested the ability of these four compounds to inhibit the enzymatic activity of either wild-type or D1228V cMET *in vitro*. All four compounds were seen to potently inhibit the activity of wild-type cMET (with  $pIC_{50}$  values beyond the theoretical tight binding limit of the assay, i.e., >8.6), though only savolitinib appeared over 100-fold less active against D1228V cMET (Figure 2f–g and Table S1). These findings are in agreement with the cellular HTRF data described above, which showed the type-II compounds foretinib and BMS-777607, but not savolitinib, to be equipotent against wild-type and D1228V cMET. To explore these findings further, we used SPR to measure the binding affinity of these four compounds for wild-type and D1228V cMET. These data showed the type-II compounds foretinib and BMS-777607 to bind with equally high (at least single-digit nanomolar) affinity to both wild-type and D1228V cMET, with the type-I compounds savolitinib and crizotinib, respectively, displaying a 66000-fold and 5-fold reduction in affinity for D1228V cMET compared to the wild-type protein (Tables S1 and S2 and Figure S1).

Although no longer in active clinical development, the potency against both wild-type and D1228V cMET seen for the type-II inhibitors studied here indicates that it is possible to design small molecule inhibitors able to simultaneously target both the D1228V and wild-type forms of cMET. However, it should be noted that type-II inhibitors typically have far broader activity profiles than type-I inhibitors,<sup>15</sup> which is associated with an expected increased risk of toxicity.<sup>16</sup> The marginal activity of crizotinib against D1228V cMET suggests that it may be possible to develop type-I inhibitors able to target both wild-type and mutant forms of the enzyme. However, whether this could be achieved while maintaining the exquisite level of selectivity seen for compounds such as savolitinib remains to be seen. It is perhaps noteworthy that crizotinib is less selective for cMET than savolitinib, with the former also seen to potently inhibit the ALK and ROS1

kinases.<sup>13,32</sup> In addition, it is worth noting that both crizotinib and the type-II inhibitors studied here may not reach the clinical exposures needed for target coverage over 24 h,<sup>33,34</sup> underscoring the need for a compound with suitable target exposure, selectivity, and potency against wild type and mutant cMET.

In order to investigate the structural effects of the D1228V point mutation at the atomic level, we sought to characterize D1228V and wild-type cMET by X-ray crystallography. The binding mode of savolitinib to wild-type cMET has not been confirmed experimentally but is assumed to be analogous to that of other type-I cMET compounds such as crizotinib, which have been shown by X-ray crystallography to bind to the hinge region of the kinase with  $\pi$ -stacking interactions with Y1230.<sup>13</sup> We therefore determined a cocrystal structure of wild-type cMET in complex with savolitinib, which confirms the expected binding mode, with the inhibitor binding to the ATP site, making hydrogen bonding interactions with the hinge region (residue M1160) and D1222, along with the characteristic  $\pi$ -stacking interaction with Y1230 of the A-loop, the orientation of which is stabilized by a key salt-bridge between D1228 and K1110 (Figure 3 and Table S3). This

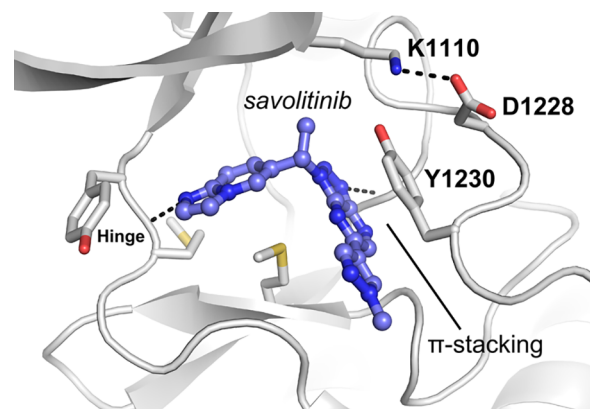


**Figure 3.** Crystal structure of wild-type cMET bound by savolitinib, highlighting the key role that residues Y1230, K1110, and D1228 play in the inhibitor binding mode.

structure therefore indicates that alteration of Y1230 either directly (through Y1230 point mutations) or indirectly (through D1228 point mutations) would be expected to reduce the ability of savolitinib to bind and inhibit cMET, which is in line with the findings described above and previously.<sup>16</sup>

Following this, we attempted to structurally characterize the D1228V cMET mutant. Apo crystallization experiments yielded no crystals, and as savolitinib was seen to be largely inactive against D1228V cMET (Figure 2 and Table S1), cocrystallization of the mutant protein with this compound was not attempted. Cocrystallization of the D1228V cMET mutant with crizotinib, however, was attempted, as SPR data indicated reasonably strong binding (albeit reduced compared to wild-type cMET) (Table S1). However, no crystals were obtained. We next turned to the type-II compounds foretinib and BMS-777607, both of which we were able to cocrystallize in complex with the D1228V cMET mutant (Table S3). The crystal structure of the D1228V cMET mutant bound by foretinib was solved to a resolution of 1.67 Å and reveals an overall inhibitor binding mode highly similar to the equivalent wild-type

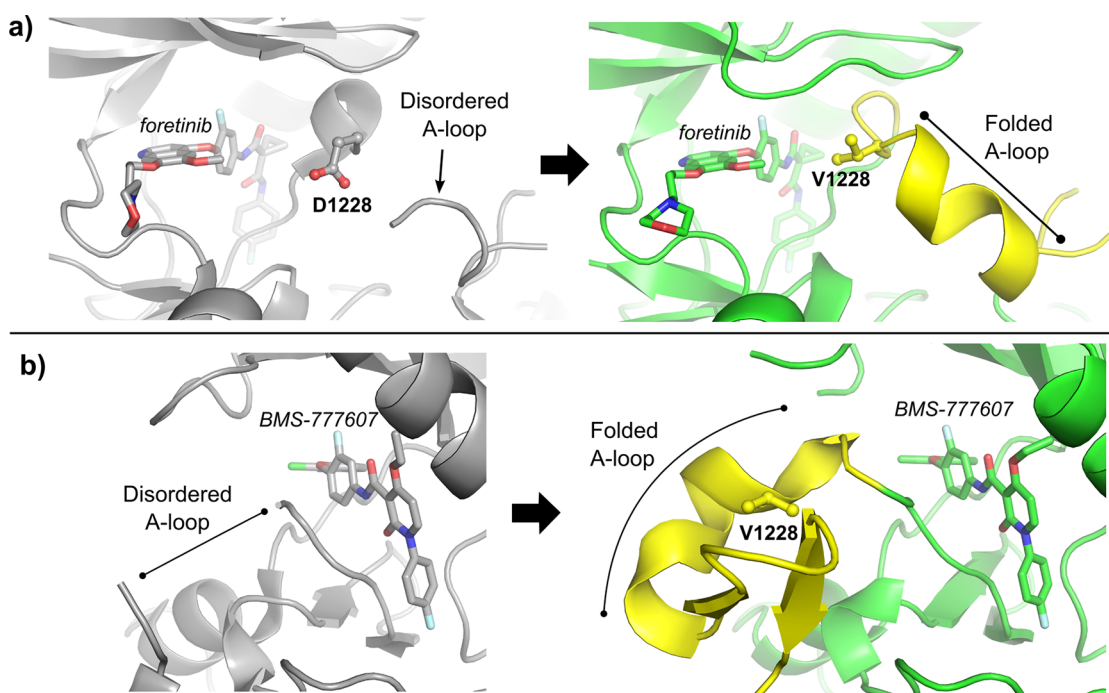


**Figure 4.** Crystal structures of D1228V cMET-inhibitor complexes. (a) Crystal structures of cMET bound by foretinib. Left panel: wild-type cMET bound by foretinib (PDB entry 3LQ8<sup>30</sup>). Right panel: D1228V cMET bound by foretinib, highlighting ordering of the A-loop (yellow). (b) Crystal structures of cMET bound by BMS-777607. Left panel: wild-type cMET bound by BMS-777607 (PDB entry 3F82<sup>31</sup>). Right panel: D1228V cMET bound by BMS-777607, highlighting ordering of the A-loop (yellow).

complex<sup>30</sup> (Figure 4a). This involves a key hydrogen bond between the quinoline core of the compound and the cMET hinge residue M1160, with the terminal fluoro-phenyl group occupying the lipophilic pocket adjacent to the  $\alpha$ C-helix created by the displacement of the highly conserved “DFG” motif. Surprisingly, however, while the crystal structure of wild-type cMET bound by foretinib shows the A-loop to be largely disordered beyond residue D1228,<sup>30</sup> the D1228V cMET crystal structure bound by foretinib reported here reveals the A-loop (which is free of crystal packing contacts) to be well-ordered, with residues 1228–1235 adopting a helical conformation (Figure 4a). Importantly, residue V1228 is resolved in electron density (Figure S2a) and is seen to be positioned such that this residue does not interact directly with foretinib, in line with the observed equipotent cellular and biochemical activity and affinity of foretinib for WT and D1228V mutant cMET (Figure 2 and Table S1).

By displacing the “DFG” motif, type-II inhibitors often cause the A-loop of cMET to be disordered (Figure S3), and we were therefore surprised to see the A-loop of the D1228V cMET mutant to adopt a well-ordered conformation when in complex with foretinib. As this ordering of the A-loop alters the protein conformation surrounding the ligand binding site of D1228V cMET relative to the wild-type complex (Figure 4a), this observation could have implications concerning inhibitor design. As a result, we sought to investigate the influence of crystal packing factors on the observed A-loop conformations. The D1228V cMET–foretinib complex reported here does not belong to the same space group and unit cell as that of the available wild-type cMET–foretinib structure;<sup>30</sup> thus, the A-loops of these structures are subject to different crystal packing environments. Fortunately, we were able to determine an additional crystal structure of wild-type cMET bound by foretinib in the same space group as that of

the D1228V cMET–foretinib complex (Table S3), enabling a valid structural comparison. This wild-type cMET–foretinib crystal structure is isomorphous with the previously reported equivalent complex<sup>30</sup> (with an RMSD of 0.857 Å for 2046 to 2046 atoms, see Figure S4) and, interestingly, reveals the A-loop to be largely disordered, suggesting that the D1228V mutation induces the observed helical conformation of the A-loop in the D1228V cMET–foretinib structure, rather than crystal packing forces.

The crystal structure of a second type-II compound, BMS-777607, bound to D1228V cMET provided further insight into the conformation and folding of this mutant (Figures 4b and S2b and Table S3). This structure reveals a typical type-II inhibitor binding mode involving hinge hydrogen bonding interactions and displacement of the “DFG” motif, analogous to the equivalent wild-type complex.<sup>31</sup> Interestingly, the A-loop of the D1228V cMET bound by BMS-777607 is well-folded and predominantly helical, contrasting starkly with the disordered A-loop of the equivalent wild-type complex (PDB entry 3F82<sup>31</sup>) (Figure 4b) and echoing the situation of foretinib bound to this same cMET mutant described above (Figure 4a). Importantly, in the D1228V cMET–BMS-777607 complex, V1228 does not directly contact the inhibitor, mirroring again the D1228V cMET–foretinib complex described above, and correlating with the observed equipotency of this type-II compound for wild-type and D1228V cMET (Figure 2 and Table S1).

The cellular and *in vitro* data we have reported here indicates clearly that savolitinib, while highly active against wild-type cMET, is over 50,000-fold less active against the D1228V cMET mutant. In addition, and in agreement with a previous report,<sup>16</sup> two type-II inhibitors were shown to be equipotent against wild-type and D1228V cMET. The crystal structures reported in this work help rationalize these observations, with

the structure of wild-type cMET bound by the type-I inhibitor savolitinib confirming the key roles that the Y1230 and D1228 A-loop residues play in the binding mode of this compound. The crystal structures of D1228V cMET bound by two different type-II compounds provide structural confirmation that the mutated residue (V1228) does not directly interact with these inhibitors, correlating with the equipotency of these compounds for wild-type and D1228V cMET. Additionally, these crystal structures indicate that the D1228V cMET mutation appears to induce conformational changes of the A-loop compared to the wild-type kinase. The mutant cMET structures reported here therefore may provide structural guidance for the design of D1228V-selective tool compounds, which would facilitate mechanistic investigations into this clinically observed resistance-conferring mutation of cMET.

If the preliminary clinical efficacy seen for type-I inhibitors such as savolitinib in settings where cMET plays a key role as a tumor driver<sup>17</sup> or resistance driver<sup>10,11</sup> is confirmed in further clinical studies, then the molecular understanding of clinically acquired resistance mechanisms such as that described here for D1228V cMET will become important areas of future clinical research.

## ■ ASSOCIATED CONTENT

### Supporting Information

The Supporting Information is available free of charge on the ACS Publications website at DOI: [10.1021/acsmchemlett.9b00276](https://doi.org/10.1021/acsmchemlett.9b00276).

Experimental procedures for cellular, biochemical and SPR studies, protein expression, and X-ray crystallography; additional figures showing SPR sensorgrams and X-ray crystal structures; tables containing *in vitro* data, SPR data analysis, and crystallographic data (PDF)

### Accession Codes

Atomic coordinates and structure factors have been deposited in the Protein Data Bank with accession codes 6SDC, 6SDD, 6SDE, and 6SD9.

## ■ AUTHOR INFORMATION

### Corresponding Authors

\*E-mail: [gavin.collie@astrazeneca.com](mailto:gavin.collie@astrazeneca.com).

\*E-mail: [ana.narvaez@astrazeneca.com](mailto:ana.narvaez@astrazeneca.com).

### ORCID

Gavin W. Collie: [0000-0002-0406-922X](https://orcid.org/0000-0002-0406-922X)

### Present Addresses

<sup>1</sup>Silicon Therapeutics, Boston, MA 02110, U.S.

<sup>#</sup>Moderna Therapeutics, Cambridge, MA 02139, U.S.

### Notes

The authors declare the following competing financial interest(s): All authors are or were employees of AstraZeneca.

## ■ ACKNOWLEDGMENTS

Thanks to the Diamond Light Source and SOLEIL synchrotrons for providing access to data collection facilities.

## ■ ABBREVIATIONS

cMET, mesenchymal-to-epithelial transition factor; NSCLC, non-small cell lung carcinoma; HEK, human embryonic kidney cells; HTRF, homogeneous time-resolved Förster resonance energy transfer; SPR, surface plasmon resonance

## ■ REFERENCES

- (1) Zhang, Y.; Xia, M.; Jin, K.; Wang, S.; Wei, H.; Fan, C.; Wu, Y.; Li, X.; Li, X.; Li, G.; Zeng, Z.; Xiong, W. Function of the c-Met receptor tyrosine kinase in carcinogenesis and associated therapeutic opportunities. *Mol. Cancer* **2018**, *17*, 45.
- (2) Oxnard, G. R.; Arcila, M. E.; Sima, C. S.; Riely, G. J.; Chmielecki, J.; Kris, M. G.; Pao, W.; Ladanyi, M.; Miller, V. A. Acquired resistance to EGFR tyrosine kinase inhibitors in EGFR-mutant lung cancer: distinct natural history of patients with tumors harboring the T790M mutation. *Clin. Cancer Res.* **2011**, *17*, 1616–1622.
- (3) Yu, H. A.; Arcila, M. E.; Rekhman, N.; Sima, C. S.; Zakowski, M. F.; Pao, W.; Kris, M. G.; Miller, V. A.; Ladanyi, M.; Riely, G. J. Analysis of tumor specimens at the time of acquired resistance to EGFR-TKI therapy in 155 patients with EGFR-mutant lung cancers. *Clin. Cancer Res.* **2013**, *19*, 2240–2247.
- (4) Arcila, M. E.; Oxnard, G. R.; Nafa, K.; Riely, G. J.; Solomon, S. B.; Zakowski, M. F.; Kris, M. G.; Pao, W.; Miller, V. A.; Ladanyi, M. Rebiopsy of lung cancer patients with acquired resistance to EGFR inhibitors and enhanced detection of the T790M mutation using a locked nucleic acid-based assay. *Clin. Cancer Res.* **2011**, *17*, 1169–1180.
- (5) Sun, J. M.; Ahn, M. J.; Choi, Y. L.; Ahn, J. S.; Park, K. Clinical implications of T790M mutation in patients with acquired resistance to EGFR tyrosine kinase inhibitors. *Lung cancer* **2013**, *82*, 294–298.
- (6) Cross, D. A.; Ashton, S. E.; Ghiorghiu, S.; Eberlein, C.; Nebhan, C. A.; Spitzler, P. J.; Orme, J. P.; Finlay, M. R.; Ward, R. A.; Mellor, M. J.; Hughes, G.; Rahi, A.; Jacobs, V. N.; Red Brewer, M.; Ichihara, E.; Sun, J.; Jin, H.; Ballard, P.; Al-Kadhimi, K.; Rowlinson, R.; Klinowska, T.; Richmond, G. H.; Cantarini, M.; Kim, D. W.; Ranson, M. R.; Pao, W. AZD9291, an irreversible EGFR TKI, overcomes T790M-mediated resistance to EGFR inhibitors in lung cancer. *Cancer Discovery* **2014**, *4*, 1046–1061.
- (7) Wu, Y. L.; Ahn, M. J.; Garassino, M. C.; Han, J. Y.; Katakami, N.; Kim, H. R.; Hodge, R.; Kaur, P.; Brown, A. P.; Ghiorghiu, D.; Papadimitrakopoulou, V. A.; Mok, T. S. K. CNS Efficacy of Osimertinib in Patients With T790M-Positive Advanced Non-Small-Cell Lung Cancer: Data From a Randomized Phase III Trial (AURA3). *J. Clin. Oncol.* **2018**, *36*, 2702–2709.
- (8) Papadimitrakopoulou, V. A.; Wu, Y.-L.; Han, J.-Y.; Ahn, M.-J.; Ramalingam, S. S.; John, T.; Okamoto, I.; Yang, J. C.-H.; Bulusu, K. C.; Laus, G.; Collins, B.; Barrett, J. C.; Chmielecki, J.; Mok, T. S. K. Analysis of resistance mechanisms to osimertinib in patients with EGFR T790M advanced NSCLC from the AURA3 study. *Ann. Oncol.* **2018**, *29*, mdy424.064.
- (9) Ramalingam, S. S.; Cheng, Y.; Zhou, C.; Ohe, Y.; Imamura, F.; Cho, B. C.; Lin, M.-C.; Majem, M.; Shah, R.; Rukazenzov, Y.; Todd, A.; Markovets, A.; Barrett, J. C.; Chmielecki, J.; Gray, J. Mechanisms of acquired resistance to first-line osimertinib: Preliminary data from the phase III FLAURA study. *Ann. Oncol.* **2018**, *29*, mdy424.063.
- (10) Sequist, L. V. TATTON Phase Ib expansion cohort: Osimertinib plus savolitinib for patients (pts) with EGFR-mutant, MET-amplified NSCLC after progression on prior third-generation epidermal growth factor receptor (EGFR) tyrosine kinase inhibitor (TKI); AACR: Atlanta, 2019.
- (11) Yu, H. TATTON Phase Ib expansion cohort: Osimertinib plus savolitinib for patients (pts) with EGFR-mutant, MET-amplified NSCLC after progression on prior first/second-generation epidermal growth factor receptor (EGFR) tyrosine kinase inhibitor (TKI); AACR: Atlanta, 2019.
- (12) Parikh, P. K.; Ghate, M. D. Recent advances in the discovery of small molecule c-Met Kinase inhibitors. *Eur. J. Med. Chem.* **2018**, *143*, 1103–1138.
- (13) Cui, J. J.; Tran-Dube, M.; Shen, H.; Nambu, M.; Kung, P. P.; Pairish, M.; Jia, L.; Meng, J.; Funk, L.; Botrous, I.; McTigue, M.; Grodzky, N.; Ryan, K.; Padrique, E.; Alton, G.; Timofeevski, S.; Yamazaki, S.; Li, Q.; Zou, H.; Christensen, J.; Mroczkowski, B.; Bender, S.; Kania, R. S.; Edwards, M. P. Structure based drug design of crizotinib (PF-02341066), a potent and selective dual inhibitor of mesenchymal-epithelial transition factor (c-MET) kinase and anaplastic lymphoma kinase (ALK). *J. Med. Chem.* **2011**, *54*, 6342–6363.

- (14) Jia, H.; Dai, G.; Weng, J.; Zhang, Z.; Wang, Q.; Zhou, F.; Jiao, L.; Cui, Y.; Ren, Y.; Fan, S.; Zhou, J.; Qing, W.; Gu, Y.; Wang, J.; Sai, Y.; Su, W. Discovery of (S)-1-(1-(Imidazo[1,2-a]pyridin-6-yl)ethyl)-6-(1-methyl-1H-pyrazol-4-yl)-1H-[1,2,3]triazolo[4,5-b]pyridazine (volitinib) as a highly potent and selective mesenchymal-epithelial transition factor (c-Met) inhibitor in clinical development for treatment of cancer. *J. Med. Chem.* **2014**, *57*, 7577–7589.
- (15) Reungwetwattana, T.; Liang, Y.; Zhu, V.; Ou, S. I. The race to target MET exon 14 skipping alterations in non-small cell lung cancer: The Why, the How, the Who, the Unknown, and the Inevitable. *Lung cancer* **2017**, *103*, 27–37.
- (16) Bahcall, M.; Sim, T.; Paweletz, C. P.; Patel, J. D.; Alden, R. S.; Kuang, Y.; Sacher, A. G.; Kim, N. D.; Lydon, C. A.; Awad, M. M.; Jaklitsch, M. T.; Sholl, L. M.; Janne, P. A.; Oxnard, G. R. Acquired METD1228V Mutation and Resistance to MET Inhibition in Lung Cancer. *Cancer Discovery* **2016**, *6*, 1334–1341.
- (17) Lu, S. Preliminary efficacy and safety results of savolitinib treating patients with pulmonary sarcomatoid carcinoma (PSC) and other types of non-small cell lung cancer (NSCLC) harboring MET exon 14 skipping mutations; AACR: Atlanta, 2019.
- (18) Dong, H. J.; Li, P.; Wu, C. L.; Zhou, X. Y.; Lu, H. J.; Zhou, T. Response and acquired resistance to crizotinib in Chinese patients with lung adenocarcinomas harboring MET Exon 14 splicing alternations. *Lung cancer* **2016**, *102*, 118–121.
- (19) Heist, R. S.; Sequist, L. V.; Borger, D.; Gainor, J. F.; Arellano, R. S.; Le, L. P.; Dias-Santagata, D.; Clark, J. W.; Engelman, J. A.; Shaw, A. T.; Iafrate, A. J. Acquired Resistance to Crizotinib in NSCLC with MET Exon 14 Skipping. *J. Thorac. Oncol.* **2016**, *11*, 1242–1245.
- (20) Kang, J.; Chen, H. J.; Wang, Z.; Liu, J.; Li, B.; Zhang, T.; Yang, Z.; Wu, Y. L.; Yang, J. J. Osimertinib and Cabozantinib Combinatorial Therapy in an EGFR-Mutant Lung Adenocarcinoma Patient with Multiple MET Secondary-Site Mutations after Resistance to Crizotinib. *J. Thorac. Oncol.* **2018**, *13*, e49–e53.
- (21) Li, A.; Yang, J. J.; Zhang, X. C.; Zhang, Z.; Su, J.; Gou, L. Y.; Bai, Y.; Zhou, Q.; Yang, Z.; Han-Zhang, H.; Zhong, W. Z.; Chuai, S.; Zhang, Q.; Xie, Z.; Gao, H.; Chen, H.; Wang, Z.; Wang, Z.; Yang, X. N.; Wang, B. C.; Gan, B.; Chen, Z. H.; Jiang, B. Y.; Wu, S. P.; Liu, S. Y.; Xu, C. R.; Wu, Y. L. Acquired MET Y1248H and D1246N Mutations Mediate Resistance to MET Inhibitors in Non-Small Cell Lung Cancer. *Clin. Cancer Res.* **2017**, *23*, 4929–4937.
- (22) Ou, S. I.; Young, L.; Schrock, A. B.; Johnson, A.; Klempner, S. J.; Zhu, V. W.; Miller, V. A.; Ali, S. M. Emergence of Preexisting MET Y1230C Mutation as a Resistance Mechanism to Crizotinib in NSCLC with MET Exon 14 Skipping. *J. Thorac. Oncol.* **2017**, *12*, 137–140.
- (23) Schrock, A. B.; Lai, A.; Ali, S. M.; Miller, V. A.; Racz, L. E. Mutation of MET Y1230 as an Acquired Mechanism of Crizotinib Resistance in NSCLC with MET Exon 14 Skipping. *J. Thorac. Oncol.* **2017**, *12*, e89–e90.
- (24) Bellon, S. F.; Kaplan-Lefko, P.; Yang, Y.; Zhang, Y.; Moriguchi, J.; Rex, K.; Johnson, C. W.; Rose, P. E.; Long, A. M.; O'Connor, A. B.; Gu, Y.; Coxon, A.; Kim, T. S.; Tasker, A.; Burgess, T. L.; Dussault, I. c-Met inhibitors with novel binding mode show activity against several hereditary papillary renal cell carcinoma-related mutations. *J. Biol. Chem.* **2008**, *283*, 2675–2683.
- (25) Chiara, F.; Michieli, P.; Pugliese, L.; Comoglio, P. M. Mutations in the met oncogene unveil a "dual switch" mechanism controlling tyrosine kinase activity. *J. Biol. Chem.* **2003**, *278*, 29352–29358.
- (26) Qi, J.; McTigue, M. A.; Rogers, A.; Lifshits, E.; Christensen, J. G.; Janne, P. A.; Engelman, J. A. Multiple mutations and bypass mechanisms can contribute to development of acquired resistance to MET inhibitors. *Cancer Res.* **2011**, *71*, 1081.
- (27) Tiedt, R.; Degenkolbe, E.; Furet, P.; Appleton, B. A.; Wagner, S.; Schoepfer, J.; Buck, E.; Ruddy, D. A.; Monahan, J. E.; Jones, M. D.; Blank, J.; Haasen, D.; Drueckes, P.; Wartmann, M.; McCarthy, C.; Sellers, W. R.; Hofmann, F. A drug resistance screen using a selective MET inhibitor reveals a spectrum of mutations that partially overlap with activating mutations found in cancer patients. *Cancer Res.* **2011**, *71*, 5255.
- (28) Timofeevski, S. L.; McTigue, M. A.; Ryan, K.; Cui, J.; Zou, H. Y.; Zhu, J. X.; Chau, F.; Alton, G.; Karlicek, S.; Christensen, J. G.; Murray, B. W. Enzymatic Characterization of c-Met Receptor Tyrosine Kinase Oncogenic Mutants and Kinetic Studies with Aminopyridine and Triazolopyridazine Inhibitors. *Biochemistry* **2009**, *48*, 5339.
- (29) Ugolini, A.; Kenigsberg, M.; Rak, A.; Vallee, F.; Houtmann, J.; Lowinski, M.; Capdevila, C.; Khider, J.; Albert, E.; Martinet, N.; Nemecek, C.; Grapinet, S.; Baque, E.; Roesner, M.; Delaisi, C.; Calvet, L.; Bonche, F.; Semiond, D.; Egile, C.; Goulaouic, H.; Schio, L. Discovery and Pharmacokinetic and Pharmacological Properties of the Potent and Selective MET Kinase Inhibitor 1-{6-[6-(4-Fluorophenyl)-[1,2,4]triazolo[4,3-b]pyridazin-3-ylsulfanyl]-benzothiazol-2-yl}-3-(2-morpholin-4-ylethyl)urea (SAR125844). *J. Med. Chem.* **2016**, *59*, 7066.
- (30) Qian, F.; Engst, S.; Yamaguchi, K.; Yu, P.; Won, K.-A.; Mock, L.; Lou, T.; Tan, J.; Li, C.; Tam, D.; Lougheed, J.; Yakes, F. M.; Bentzien, F.; Xu, W.; Zaks, T.; Wooster, R.; Greshock, J.; Joly, A. H. Inhibition of tumor cell growth, invasion, and metastasis by EXEL-2880 (XL880, GSK1363089), a novel inhibitor of HGF and VEGF receptor tyrosine kinases. *Cancer Res.* **2009**, *69*, 8009.
- (31) Schroeder, G. M.; An, Y.; Cai, Z.-W.; Chen, X.-T.; Clark, C.; Cornelius, L. A. M.; Dai, J.; Gullo-Brown, J.; Gupta, A.; Henley, B.; Hunt, J. T.; Jeyaseelan, R.; Kamath, A.; Kim, K.; Lippy, J.; Lombardo, L. J.; Manne, V.; Oppenheimer, S.; Sack, J. S.; Schmidt, R. J.; Shen, G.; Stefanski, K.; Tokarski, J. S.; Trainor, G. L.; Wautlet, B. S.; Wei, D.; Williams, D. K.; Zhang, Y.; Zhang, Y.; Fargnoli, J.; Borzilleri, R. M. Discovery of N-(4-(2-Amino-3-chloropyridin-4-yloxy)-3-fluorophenyl)-4-ethoxy-1-(4-fluorophenyl)-2-oxo-1,2-dihydropyridine-3-carboxamide (BMS-777607), a Selective and Orally Efficacious Inhibitor of the Met Kinase Superfamily. *J. Med. Chem.* **2009**, *52*, 1251.
- (32) Awad, M. M.; Katayama, R.; McTigue, M.; Liu, W.; Deng, Y.-L.; Brooun, A.; Friboulet, L.; Huang, D.; Falk, M. D.; Timofeevski, S.; Wilner, K. D.; Lockerman, E. L.; Khan, T. M.; Mahmood, S.; Gainor, J. F.; Digumarthy, S. R.; Stone, J. R.; Mino-Kenudson, M.; Christensen, J. G.; Iafrate, A. J.; Engelman, J. A.; Shaw, A. T. Acquired resistance to crizotinib from a mutation in CD74–ROS1. *N. Engl. J. Med.* **2013**, *368*, 2395.
- (33) Kurata, Y.; Miyauchi, N.; Suno, M.; Ito, T.; Sendo, T.; Kiura, K. Correlation of plasma crizotinib trough concentration with adverse events in patients with anaplastic lymphoma kinase positive non-small-cell lung cancer. *J. Pharm. Health Care Sci.* **2015**, *1*, 8.
- (34) Naing, A.; Kurzrock, R.; Adams, L. M.; Kleha, J. F.; Laubscher, K. H.; Bonate, P. L.; Weller, S.; Fitzgerald, C.; Xu, Y.; LoRusso, P. M. A comparison of the pharmacokinetics of the anticancer MET inhibitor foretinib free base tablet formulation to bisphosphate salt capsule formulation in patients with solid tumors. *Invest. New Drugs* **2012**, *30*, 327.